Coexistence of Spin Density Waves and Superconductivity in $(TMTSF)_2PF_6$

Arjun Narayanan,[1,*] Andhika Kiswandhi,[2] David Graf,[2] James Brooks,[2] and Paul Chaikin[1]
[1]*Department of Physics, New York University, New York 10003, USA*
[2]*National High Magnetic Field Lab, Florida State University, Tallahassee 32310, USA*
(Received 8 December 2013; published 8 April 2014)

We present simultaneous measurements of angular-dependent magnetoresistance and thermopower along all three crystal axes in $(TMTSF)_2PF_6$ for pressures to 7.4 kbar and magnetic fields to 35 T. $(TMTSF)_2PF_6$ under pressure shows the coexistence of spin density wave and metal-superconducting orders. We suggest that this coexistence results neither in microscopic coexistence nor in a new soliton wall phase, contrary to previous suggestions, but in phase separation into domains of the high-pressure metal and the low-pressure spin density wave phases. Simultaneous measurement of transport along all crystal axes allows us to unambiguously describe the domain structure, whereas the superconducting transition temperature and four independent Fermi surface-sensitive magnetoresistance signatures allow us to unambiguously characterize the coexisting metallic domains.

DOI: 10.1103/PhysRevLett.112.146402 PACS numbers: 71.27.+a, 74.25.Ld

One of the most ubiquitous set of questions for strongly correlated materials relates to the meeting of antiferromagnetic and metallic—often superconducting (SC)—order in a phase diagram. When these orders overlap, do they coexist, compete, or result in new phases? These questions arise in the cuprates, pnictides, heavy fermion superconductors, and the Bechgaard salts among others. There is no consensus in most of these material classes. However, in $(TMTSF)_2PF_6$, the situation is more promising. The measurements reported here constitute strong evidence that coexistence in the Bechgaard salts results in phase separation into alternating macroscopic domains of high-pressure metallic phase and low-pressure spin density wave (SDW) phase with domains that are aligned with the lattice.

The archetypical Bechgaard salt $(TMTSF)_2PF_6$ exhibits the phase diagram shown in Fig. 1(a). In the SDW-SC overlap region from ~5 to 6 kbar, previous evidence for coexistence exists from the simultaneous NMR and resistivity measurements of Lee *et al.* [1] and transport measurements [2]. Recently, Kang *et al.* reported a particular domain structure [3]. They observed that as pressure was increased, superconductivity developed first along the least conducting c axis only. In Fig. 1 we show our redrawing of their phase diagram with some differences [4]. With increasing pressure, the SDW transition temperature falls and at pressure P_0 metallic islands start to form [Fig. 1(b)]]. Only the c axis resistivity ρ_c shows a partial superconducting drop at 1 K before rising again as $T \to 0$. The a and b axis resistivity ρ_a, ρ_b remain insulating with increasing pressure. Near P_1, these metallic islands coalesce into pillars along the c axis leaving the c axis superconducting, and ρ_b shows a partial drop before rising at lower temperatures while ρ_a stays insulating. At P_2, the superconducting pillars form slabs in the b-c plane leaving only the a axis insulating. ρ_a shows a drop at 1 K before rising again at lower temperatures, suggesting series combination of SDW and SC domains. Finally, at P_c we have uniform superconductivity.

We confirmed and complemented the particular domain structure in Ref. [3] by performing all experiments on

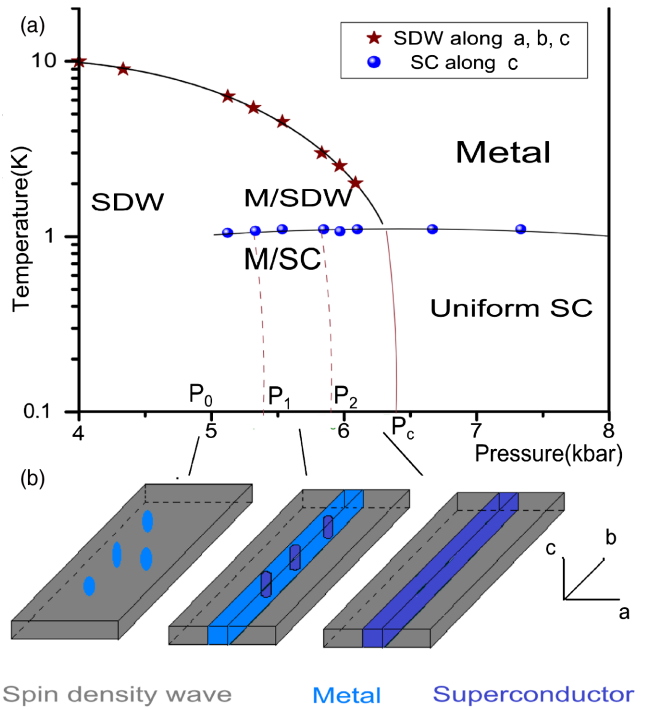

FIG. 1 (color online). (a) Phase diagram of $(TMTSF)_2PF_6$ showing low-pressure SDW, high-pressure metal (M)-SC, and the coexistence regime. The SDW transition occurs simultaneously along all axes (brown stars); SC transitions plotted (blue circles) are measured along the c axis. (b) Depiction of pressure evolution of metallic domains as described in text.

pieces of the same crystal mounted in the same pressure cell and measured during the same cool down. This allowed us to eliminate any objections with respect to pressure comparisons. We measured both anisotropic resistance and anisotropic thermopower. The question of what metal phase formed in the metallic domains of the coexistence regime is our main concern. A spatially homogenous semimetallic SDW phase, with incomplete nesting and metallic pockets on the Fermi surface [5], may be ruled out as the NMR and resistance measurements of Ref. [1] established inhomogeneous coexistence. A second scenario is macroscopic phase separation into domains of the usual high-pressure metallic phase and the low-pressure SDW phase [1,2]. The soliton model [6] is a third possibility, where a soliton wall oriented perpendicular to the a axis was thought to arise between two SDW domains with different nesting vectors. This soliton wall would be metallic. The natural orientation of the soliton walls, being along the b-c plane, fit well with the details of the observed anisotropy, namely, that superconductivity arose perpendicular to the a axis. This similarity led previous authors to suggest the soliton model to explain the metallic regions [3,5,7]. While this would naturally explain the orientation of the metal regions, the soliton wall would be a distinct two-dimensional metal, existing in slabs of thickness $\sim\xi_{\mathrm{sdw}}$. It would have distinct properties from the high-pressure metal. The high-pressure metal phase is well studied, and we concentrate on five unique signatures of its Fermi surface: the field-induced spin density waves (FISDW) [8], the rapid oscillations (RO), the SC transition temperature, the Lebed oscillations (LO), [9] and the Danner-Kang-Chaikin (DKC) oscillations [10]. The main result of this Letter is that these signatures persist in the coexistence regime and identify the metallic domains as macroscopic and identical to the high-pressure metal.

For our first set of experiments, we measured samples of $(\mathrm{TMTSF})_2\mathrm{PF}_6$ pressurized in beryllium copper piston cylinder cells. In each pressure cell, we mounted three pieces cut from the same crystal. The crystals were grown by standard electrocrystallization techniques. The three pieces were contacted to measure ρ_a, ρ_b, and ρ_c, respectively. Contact was established by evaporating 60—100 nm gold pads on the appropriate crystal faces. The mounting stage also included a 100 Ω thin film heater and thermocouple, which enabled us to set up a temperature gradient along the axis of the cell. Thus, we could measure the thermopower S_a, S_b, and S_c on the samples used to measure ρ_a, ρ_b, and ρ_c, respectively, all at the same pressure. An induction coil filled with lead was included *in situ* to calibrate the pressure at low temperatures.

Figure 2 shows resistance (bottom panel) and thermopower (top panel) in a cell at 5.8 kbar. On cooling, the high-temperature metallic behavior along all three crystal axes is replaced by a gradual resistance increase signaling the SDW transition. This occurs along all three axes over a

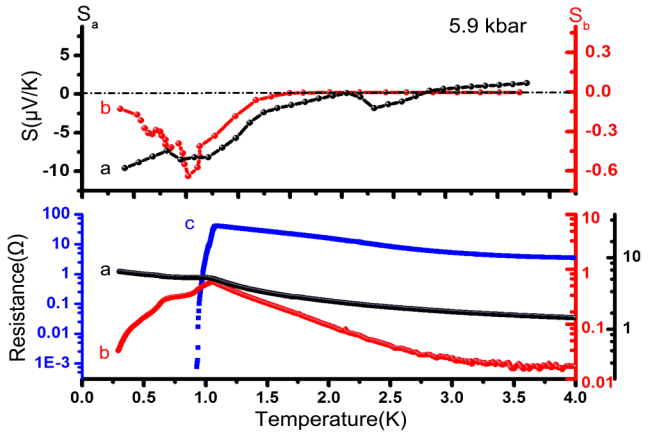

FIG. 2 (color online). Thermopower (top) along a and b axes and resistance (bottom) along all three axes in a cell at 5.9 kbar.

temperature range of 2 K. The usual S-shaped sharp SDW transition in these salts is smeared out. The thermopower anomaly in S_a at 2.5 K most clearly marks the transition. This anomaly has precisely the shape expected from previous reports for the SDW transition along the a axis; however, the related SDW transition features in S_b are suppressed [11]. This suggests that the usual SDW transition occurs in the crystal and, furthermore, that the SDW thermopower signature is shorted out for the b axes. At lower temperatures, a sharp SC transition is seen in ρ_c, a broad transition in ρ_b, while ρ_a, after a small dip, continues to increase. The c axis resistive transition is complete, and the b axis shows a double-hump transition as previously reported [3]. The anisotropy also exists in the thermopower. The absolute value of S_b is small ($< 1\ \mu\mathrm{V/K}$) consistent with a metal. Furthermore, S_b show metallic-SC behavior $S \to 0$ as $T \to 0$ below 1 K. The thermopower in the a axis direction is large ($\sim 10\ \mu\mathrm{V/K}$) and shows semiconducting behavior. Both the resistive transition and the drop in S_b move to lower temperatures by the application of magnetic field. The critical field dependence as derived from the resistive and thermopower transitions is consistent with an extrapolation of the trends at higher pressures [12]. The evolution of the anisotropy with pressure was also followed. Near 4.5 kbar, metallic and SC behavior are seen only along the c axis while the b and a axes are insulating. By 5.5 kbar, b also shows metallic and SC behavior, and then finally above 6.5 kbar we have a homogenous metal. Since we measure all three axes in the same cell, we conclude that at exactly the same pressure, both conductivity and thermopower along the three axes are different. The thermopower anisotropy above the SC transition also suggests that domains of metal and SDW coexist before the onset of SC: for example, S_c, S_b are an order of magnitude less than S_a in the range $T_c < T < T_{\mathrm{sdw}}$.

Next, we turn to the identification of the individual domains. Figure 3 shows the c axis magnetoresistance in a pressure cell at 5.9 kbar. This pressure cell was the highest

pressure we attained while remaining in the coexistence regime; however, all oscillations reported here have been observed in pressure cells at 5.4, 5.6, 5.9, and 6.1 kbar (corresponding to SDW transition temperatures from 7 to 2 K). As seen in Fig. 3, there are two sets of oscillations. The first occurs after an onset field of ~2 T and follows a Shubnikov–de Haas (SdH) behavior with a characteristic frequency of ~60 T and a nonsinusoidal shape. The second has a sinusoidal shape with characteristic frequency of ~260 T and a maximum amplitude at 2 K before being suppressed at low temperatures. There are two known oscillations in the high-pressure metal phase. First, the FISDW, which are actually transitions to SDW states that occur periodically in $1/B$ [13]. After having reached the final FISDW, that is, after having been induced by the field into the fully gapped SDW phase, the rapid oscillations RO commence at a SdH frequency of 270 T [14] and are a thermally activated breakdown oscillation. The frequency of FISDW is a measure of the so-called unnesting transfer integral, the warping of the Fermi surface that leads to suppression of nesting. The temperature and pressure dependencies of the oscillation frequencies observed in the coexistence regime are exactly as expected from a simple extrapolation of the high-pressure metallic phase behaviors for FISDW and RO, respectively. This is shown for the FISDW in Fig. 3(d). Neither of these oscillations is expected in a soliton model. Consecutive FISDW nesting wavelength differs by a length scale ~1 μm at 2 T (along the a axis) determined by the lattice constant b and the magnetic field as $l_B = \hbar/ebH$. A solitonic domain wall on the other hand must have a thickness of the order of the SDW coherence length, which is ~30 nm in these salts.

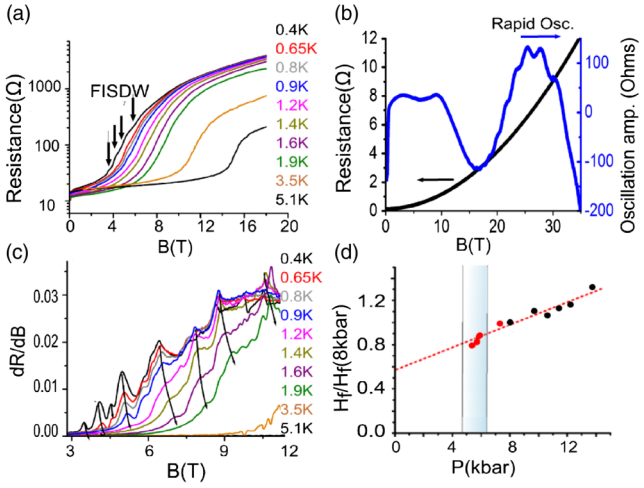

FIG. 3 (color online). (a) Longitudinal MR along c axis (5.9 kbar). (b) Background subtraction of MR showing RO at high fields (5.7 kbar). (c) Black arrows showing temperature evolution of FISDW transitions from (a). (d) Pressure evolution of FISDW frequency normalized to 8 kbar—current work (red) and previously published data (black).

There is not enough room in a soliton wall for FISDW at 2 T. The FISDW and the RO are the first two fingerprints of the high-pressure metal found to persist in the coexisting metallic domains below P_c. The third signature of the high-pressure metal is its superconducting transition temperature. The fact that the transition temperature is essentially unchanged in a 1.5 kbar region of the coexistence phase is strong evidence for phase separation. It is highly unlikely that a new soliton metal with its own unique Fermi surface dispersion and interactions would have the same superconducting T_c value as the "normal" high-pressure metal. In fact, even when ρ_c only shows a small drop due to the first onset of superconducting inclusions, the drop is precisely at 1 K. This can be seen in our phase diagram in Fig. 1 and constitutes a difference from previously published results [4].

We also conducted angular-dependent magnetoresistance (AMR) measurements. The known AMR oscillations in the high-pressure phase include LOs for rotations in the b-c plane as well as DKC oscillations for rotations in the a-c plane. The LOs appear as resistance minima at field-independent "magic angles" for which a quasiclassical electron orbit becomes commensurate for the k_b and k_c directions [9]. They are, thus, a measure of the shape of the Brillouin zone. The data are shown in Fig. 4. In Fig. 4(a), we show the Lebed oscillations (b-c rotations) in the coexistence phase at various fields. Figure 4(b) compares

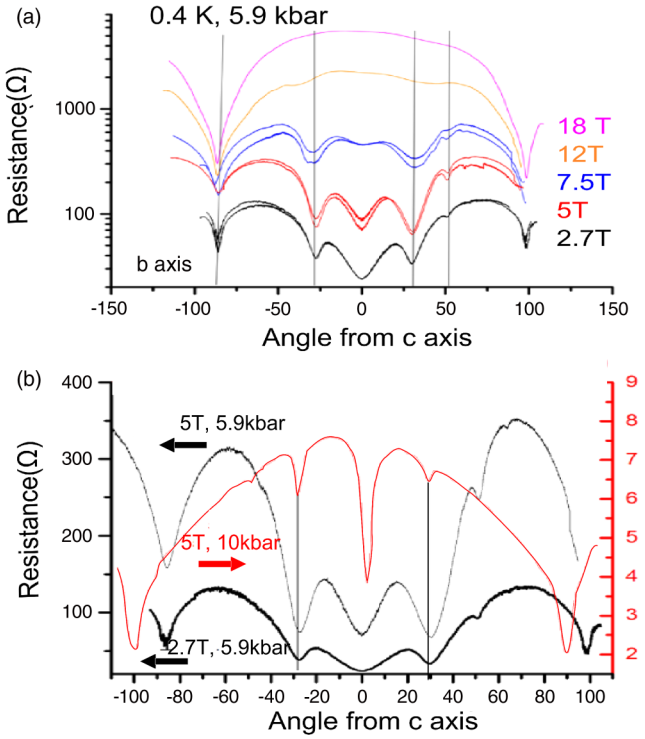

FIG. 4 (color online). (a) Lebed oscillations (b-c rotations measuring R_{zz}) at 5.9 kbar. (b) Comparison of 10 kbar Lebed oscillations [15] (red) and 5.9 kbar Lebed oscillations (black).

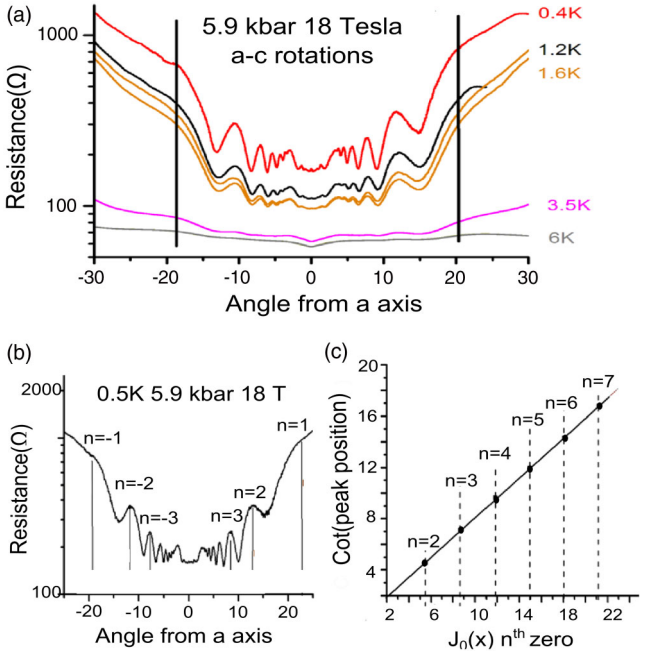

FIG. 5 (color online). (a) *a-c* rotations at various temperatures 18 T and 5.9 kbar (measuring $R_z z$). (b) *a-c* oscillations at 0.5 K with peak positions marked. (c) Cotangent of peak positions versus zeroes of Bessel function. Straight line implies that the oscillations follow the usual semiclassical description of DKC oscillations in the coexistence region.

the coexistence phase data to previously published high-pressure data. The angles are unchanged, suggesting that there is no change in the Brillouin zone shape. The DKC effect arises as resistance peaks at certain angles in the *a-c* plane, where the corresponding electron trajectories have zero average velocity along the *c* direction. The tangent of these angles is a measure of the transfer integral t_b along the *b* direction and is given by $\tan\theta_n = (2t_b c)/\gamma_n \hbar v_f$ where γ_n are the zeroes of the bessel function J_0 [10]. Figure 5(a) shows DKC oscillations at various temperatures. Note that oscillations are present as high as 6 K well above the SDW transition and the peak positions are unchanged on passing through T_{sdw}. In Figs. 5(b) and 5(c), we show that the DKC oscillation peaks occur at angles whose cotangent is proportional to the zeroes of the Bessel function J_0. This is exactly as expected for the DKC oscillations of the high-pressure metal from semiclassical electron motion [15]. The extracted value of t_b from our data is 45 meV.

In conclusion, we have used resistivity, thermopower, and Fermi surface-sensitive angular-dependent magnetotransport to clarify the coexistence of SDW and SC orders in $(\mathrm{TMTSF})_2\mathrm{PF}_6$. We characterize the metallic domain through signatures of its Fermi surface, the superconducting transition temperature, the FISDW, the rapid oscillations, and two AMR effects. This suggests that the coexistence occurs through macroscopic phase separation on the length scale of at least 1 μm. The restrictions provided by T_c and four independent Fermi surface signatures determine the metallic domains to be indistinct in any way from the high-pressure metal. A solitonic model was attractive primarily because it predicted the metallic domain walls perpendicular to the most conducting axis as experimentally observed. However, phase separation could yield the same domain geometry when the elastic energy cost of a domain wall is considered. Finally, we would like to comment on the links to other materials. In the Bechgaard salts and pnictides, unlike in the cuprates or heavy fermion systems, the suppression of nesting controls the phase diagram. This makes the organics a good candidate for comparison with the pnictides. In the pnictides, a SDW phase must be suppressed to access superconductivity, but the details of the suppression of the SDW phase are unclear. The Bechgaard salts are clean, stoichiometric materials with simple electronic structure. That the SDW phase spontaneously phase separates at the edge of its stability, into macroscopic SDW and metal domains, is likely to be of relevance. The heavy fermion superconductor CeRhIn_5 has recently been reported to display superconductivity first along the least conducting direction as pressure is tuned [16]. Even the Bechgaard salt $(\mathrm{TMTSF})_2\mathrm{ClO}_4$ has shown domain structure, but this time with cooling rate as the tuning parameter [17].

We thank V. Yakovenko and L. P. Gorkov for discussions. The work at NYU was supported by NSF MRSEC-DMR-0820341, at FSU by NSF-DMR 1005293, and the work at the NHMFL by the NSF and the state of Florida through Agreement DMR0654118.

*an859@nyu.edu; arjun.narayanan@physics.oxford.ac.uk

[1] I. J. Lee, S. E. Brown, W. Yu, M. J. Naughton, and P. M. Chaikin, Phys. Rev. Lett. **94**, 197001 (2005).
[2] T. Vuletic, P. Auban-Senzier, C. Pasquier, S. Tomic, D. Jerome, M. Heritier, and K. Bechgaard, Eur. Phys. J. B **25**, 319 (2002).
[3] N. Kang, B. Salameh, P. Auban-Senzier, D. Jerome, C. R. Pasquier, and S. Brazovskii, Phys. Rev. B **81**, 100509 (2010).
[4] Unlike in Ref. [3] we never see the SC T_c phase boundary drop below 1 K at any pressure.
[5] L. P. Gor'kov and P. D. Grigoriev, Phys. Rev. B **75**, 020507 (2007); Europhys. Lett. **71**, 425 (2005); P. D. Grigoriev, Phys. Rev. B **77**, 224508 (2008).
[6] S. A. Brazovskii, L. P. Gor'kov, and R. Schrieffer, Phys. Scr. **25**, 423 (1982); L. P. Gor'kov and P. D. Grigoriev, Europhys. Lett. **71**, 425 (2005).
[7] A. Ardavan, S. Brown, S. Kagoshima, K. Kanoda, K. Kuroki, H. Mori, M. Ogata, S. Uji, and J. Wosnitza, J. Phys. Soc. Jpn. **81**, 011004 (2012).
[8] W. Kang, S. T. Hannahs, and P. M. Chaikin, Phys. Rev. Lett. **70**, 3091 (1993).
[9] A. G. Lebed, J. Phys. I (France) **4**, 351 (1994).

[10] G. M. Danner, W. Kang, and P. M. Chaikin, Phys. Rev. Lett. **72**, 3714 (1994).
[11] K. Mortensen and E. M. Engler, Phys. Rev. B **29**, 842 (1984).
[12] I. J. Lee, P. M. Chaikin, and M. J. Naughton, Phys. Rev. Lett. **88**, 207002 (2002).
[13] P. M. Chaikin, Phys. Rev. B **31**, 4770 (1985); L. P. Gor'kov and A. G. Lebed, J. Phys. (Paris), Lett. **45**, 433 (1984).
[14] A. Kornilov, V. M. Pudalov, A. Klehe, A. Ardavan and J. S. Qualls, JETP Lett. **84**, 628 (2007); S. Uji, T. Terashima, H. Aoki, J. Brooks, M. Tokumoto, S. Takasaki, J. Yamada, and H. Anzai, Phys. Rev. B **53**, 14399 (1996).
[15] W. Kang, S. T. Hannahs, and P. M. Chaikin, Phys. Rev. Lett. **69**, 2827 (1992); G. M. Danner, W. Kang, and P. M. Chaikin, Phys. Rev. Lett. **72**, 3714 (1994).
[16] T. Park, H. Lee, I. Martin, X. Lu, V. A. Sidorov, K. Gofryk, F. Ronning, E. D. Bauer, and J. D. Thompson, Phys. Rev. Lett. **108**, 077003 (2012).
[17] Ya. A. Gerasimenko, V. A. Prudkoglyad, A. V. Kornilov, S. V. Sanduleanu, J. S. Qualls, and V. M. Pudalov, JETP Lett. **97**, 419 (2013).